

Application of Zinc Selenide and its Graphitic Carbon Nitride Composite Materials in Photocatalytic Degradation of Crystal Violet and Electrocatalytic Reduction of CO₂

科學教育與應用學系 四年級 劉予諳 指導教授 陳錦章 蔡惠燕 教授

Abstract

A combination of graphitic carbon nitride and zinc selenide was used to synthesize composite materials through hydrothermal reactions. Various proportions of the two materials were used to create different composites, which were then characterized using multiple instruments including XRD, FE-TEM, FT-IR, SEM-EDS, UV–Vis DRS, PL, EPR, HR-XPS, and BET. To test the photocatalytic efficiency of the synthesized composites, degradation experiments were conducted using crystal violet. Among the zinc selenide composite materials, ZnSe/g-C₃N₄-5wt% demonstrated the highest degradation efficiency. Electrochemical experiments were conducted to investigate the electrocatalytic reduction of carbon dioxide by suspending the zinc selenide composite materials coating them onto the surface of a graphite rod serving as the working electrode. Cyclic voltammetry tests were carried out to identify the optimal catalyst and reduction potential. The superior composite material identified was ZnSe/g-C₃N₄-5wt%. Under constant potential conditions at -0.5 V, -0.7 V, and -0.9 V, the reduction of carbon dioxide in an alkaline solution was conducted for 1 hour. The resulting products were analyzed using GC-FID. Preliminary findings suggest that the ZnSe/g-C₃N₄-5wt% composite demonstrates outstanding electrocatalytic performance. Electrocatalytic reduction of carbon dioxide at lower voltages predominantly yields acetone, and further confirmation through GC/MS is under investigation.

Result and Discussion

XRD

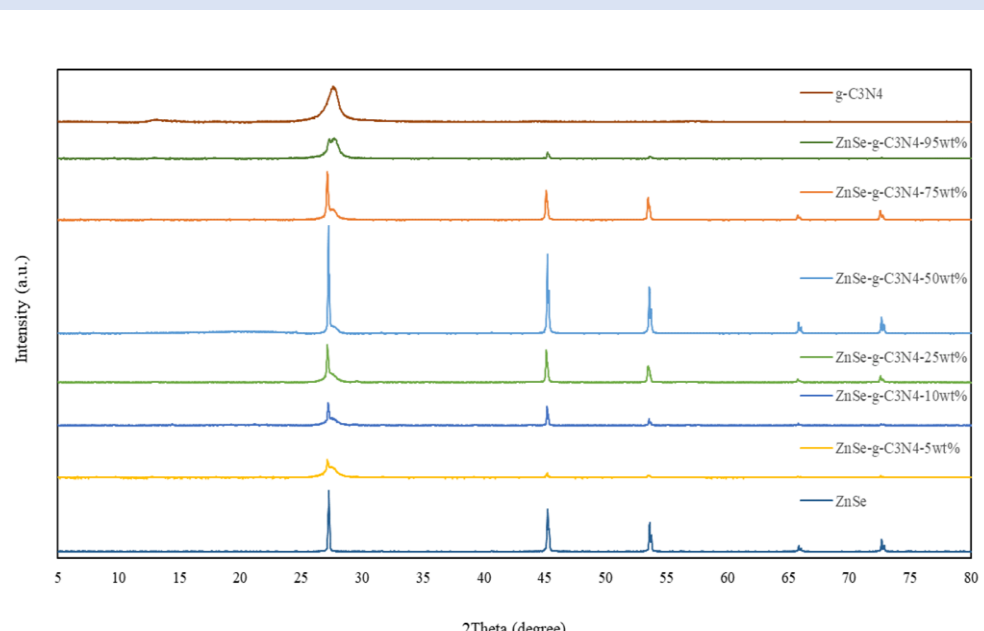


Fig. 1 XRD patterns of ZnSe composites using different content of g-C₃N₄.

FE-SEM-EDS

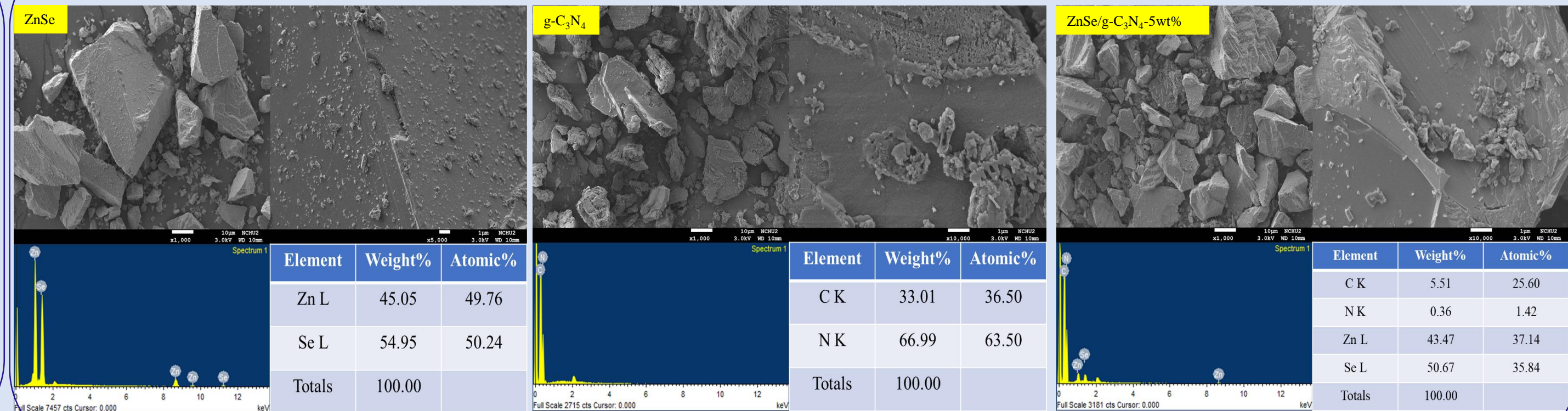


Fig. 2 FE-SEM images and EDS of ZnSe, g-C₃N₄ and ZnSe/g-C₃N₄-5wt% .

FE-TEM-EDS

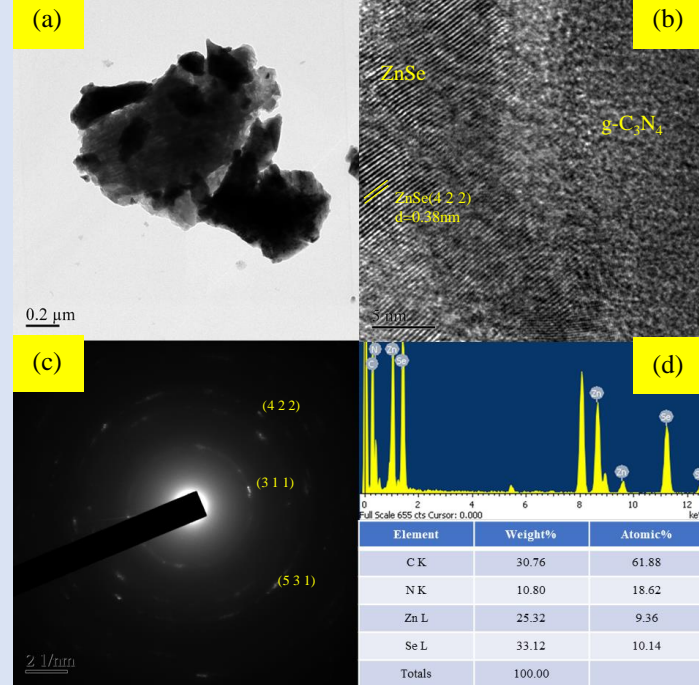


Fig. 3 (a) FE-TEM image, (b) HR-TEM image, (c) SAED and (d) EDS of ZnSe/g-C₃N₄-5wt%.

FT-IR

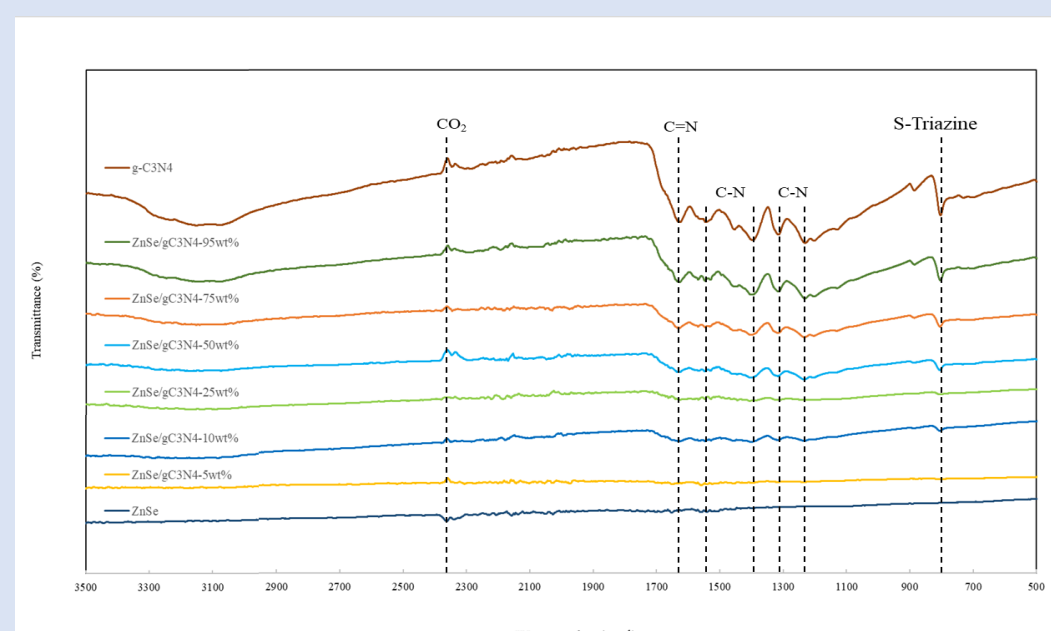


Fig. 4 FT-IR spectra of ZnSe/g-C₃N₄ in different content of g-C₃N₄.

HR-XPS

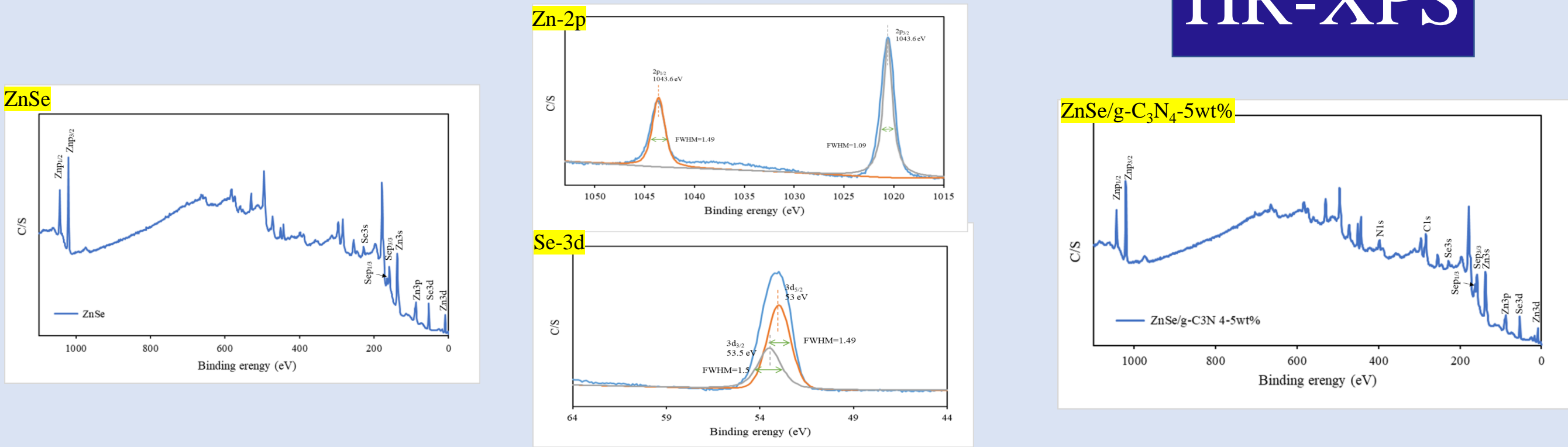
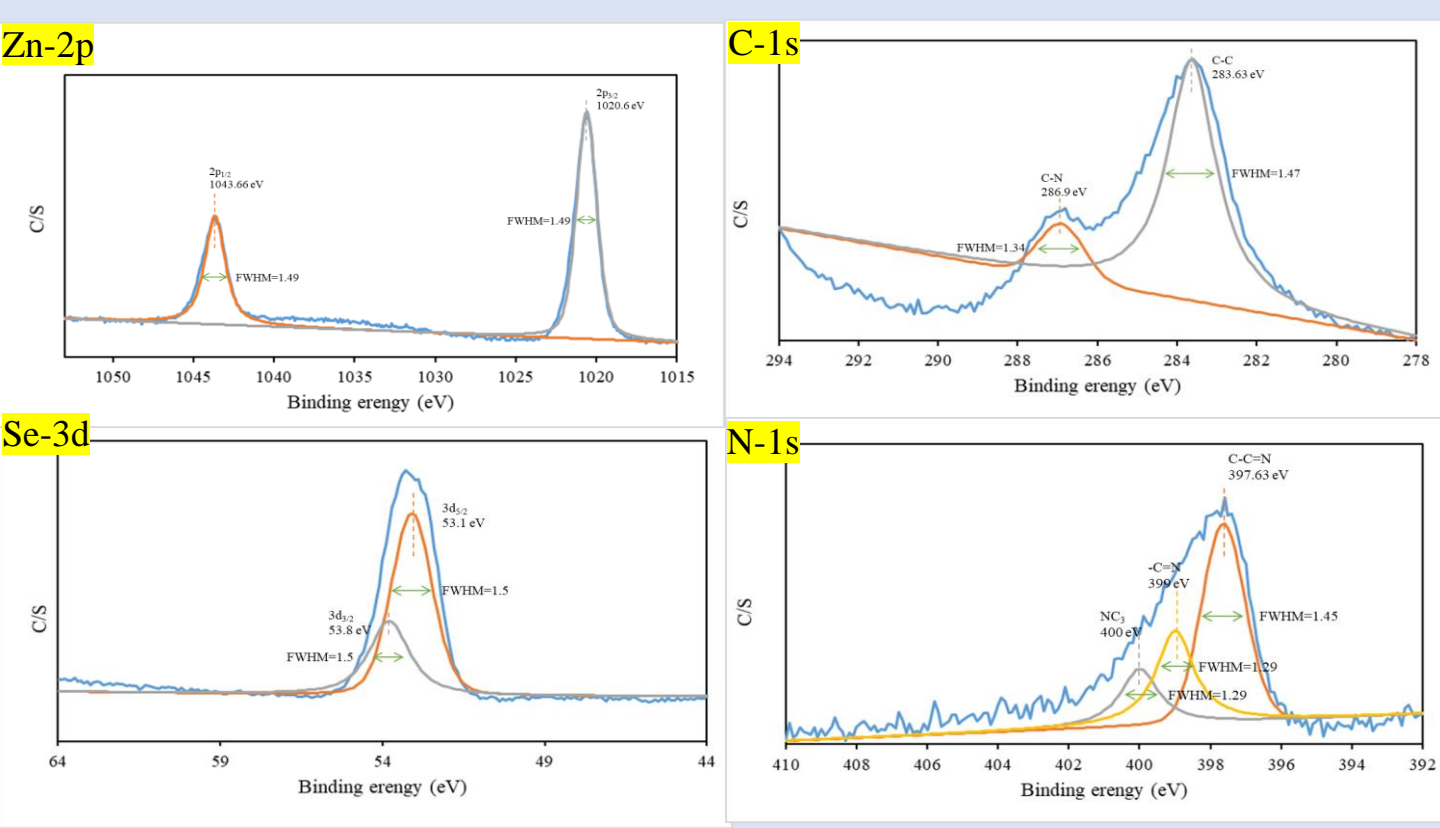


Fig. 5 HR-XPS patterns of ZnSe and ZnSe/g-C₃N₄-5wt%.



DR-UV-Vis

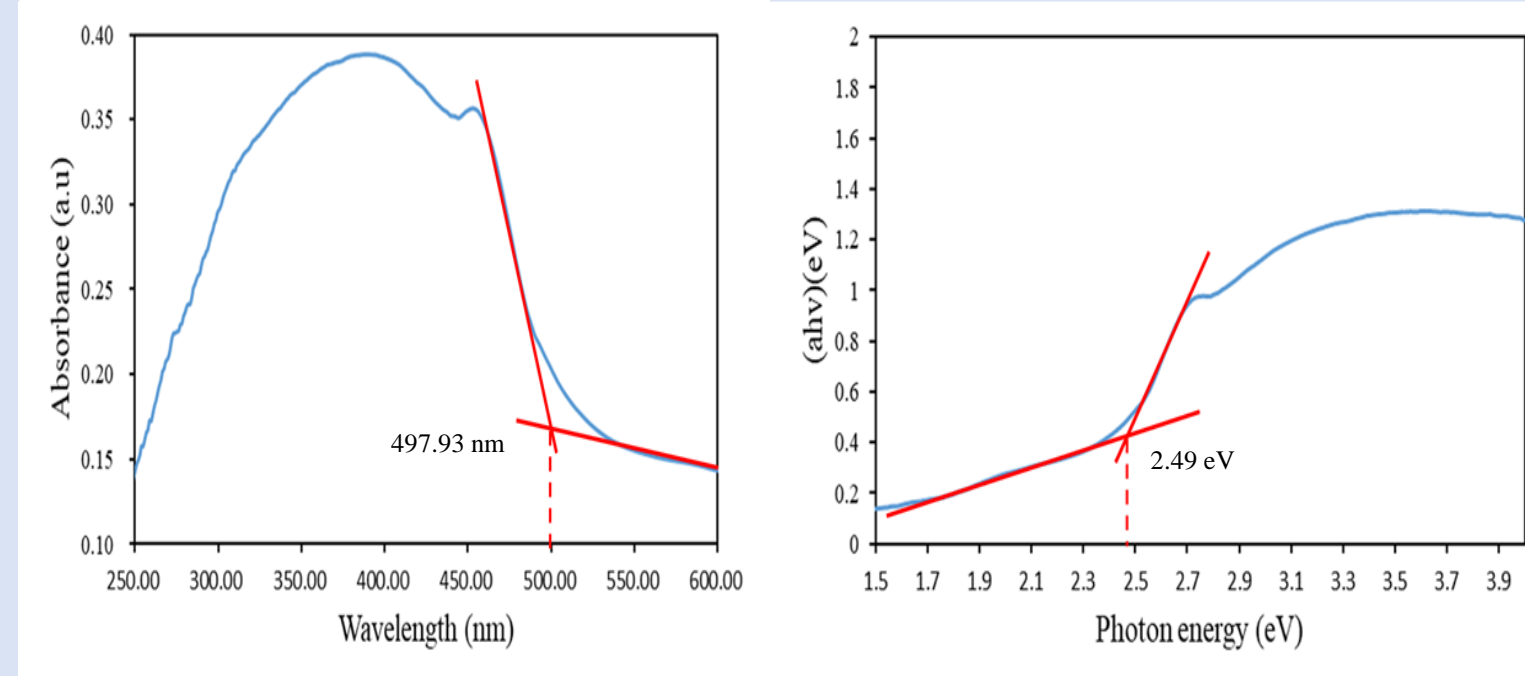


Fig. 6 DRS patterns of ZnSe/g-C₃N₄-5wt%.

Photocatalytic degradation of CV

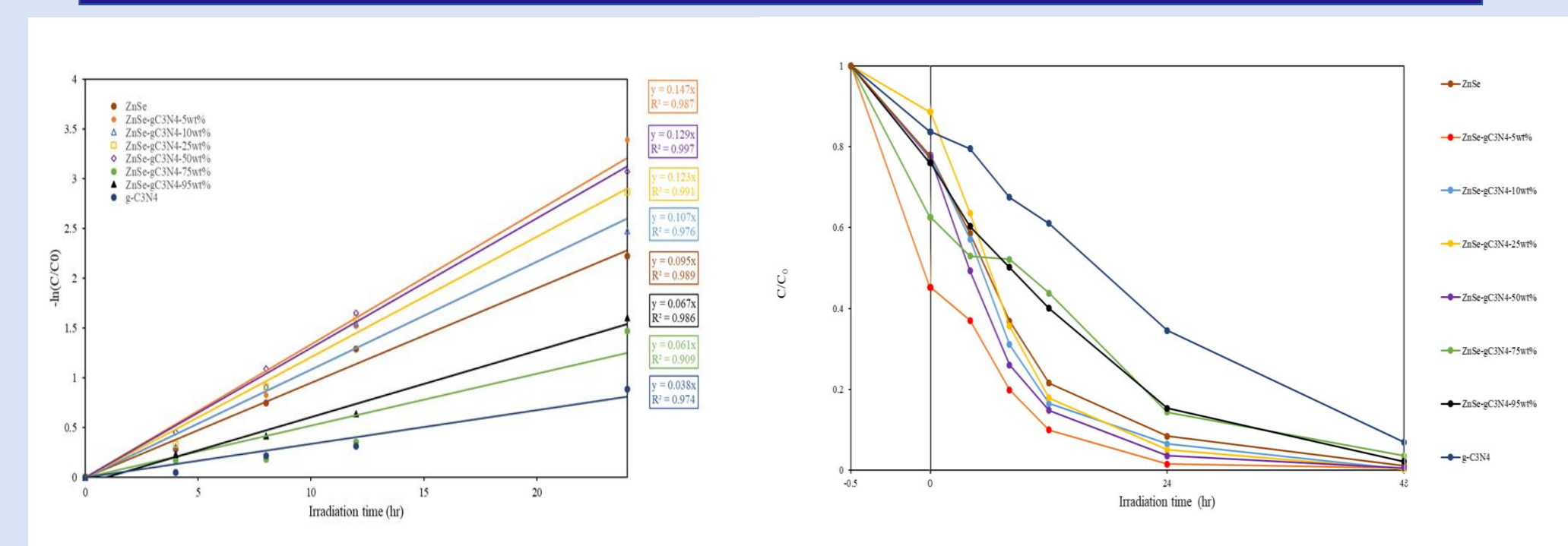


Fig. 7 Photodegradation of CV as a function of irradiation time over different ZnSe/g-C₃N₄.

PL

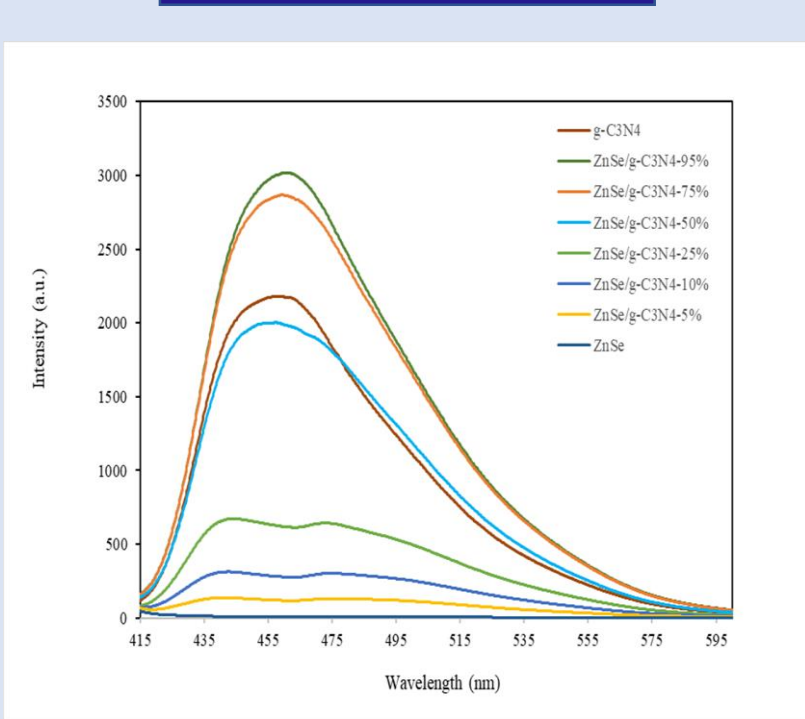


Fig. 8 PL patterns of ZnSe/ g-C₃N₄.

BET

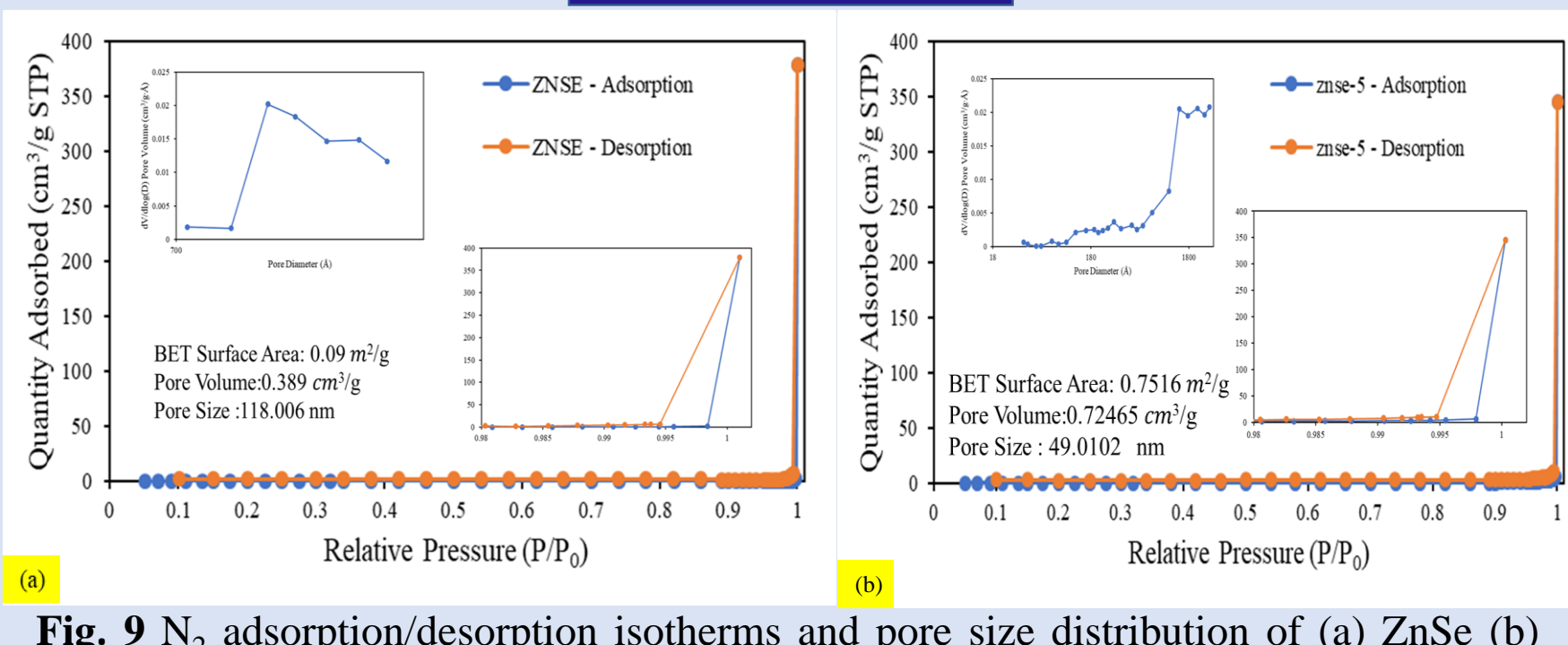


Fig. 9 N₂ adsorption/desorption isotherms and pore size distribution of (a) ZnSe (b) ZnSe /g-C₃N₄-5wt%.

Scavenger effect

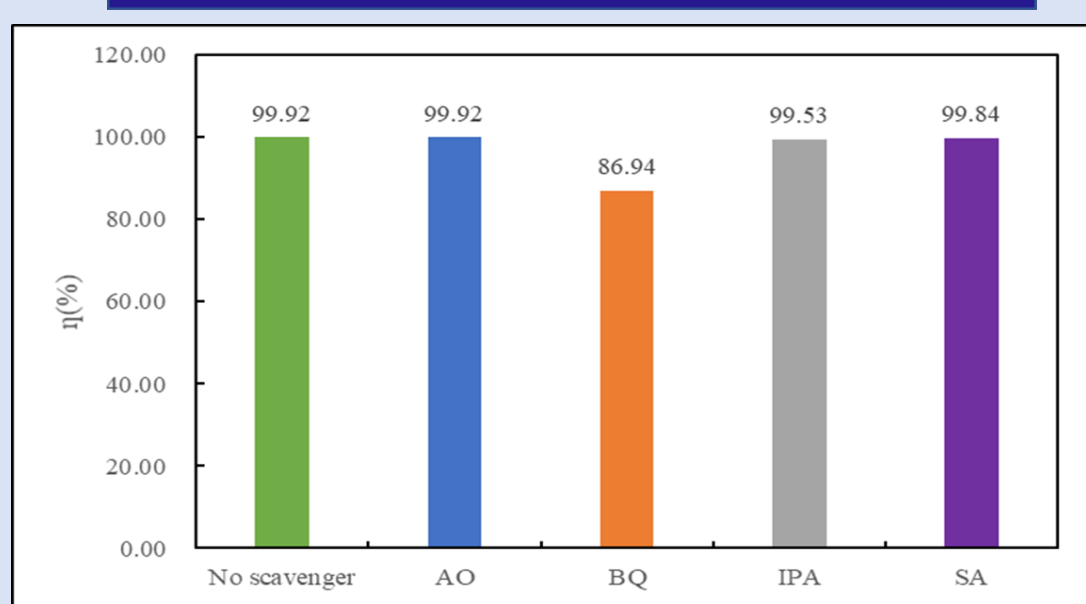


Fig. 10 The dye concentration during photodegradation as a function of irradiation time observed in ZnSe/g-C₃N₄-5wt% photocatalysts.

Electrocatalytic reaction

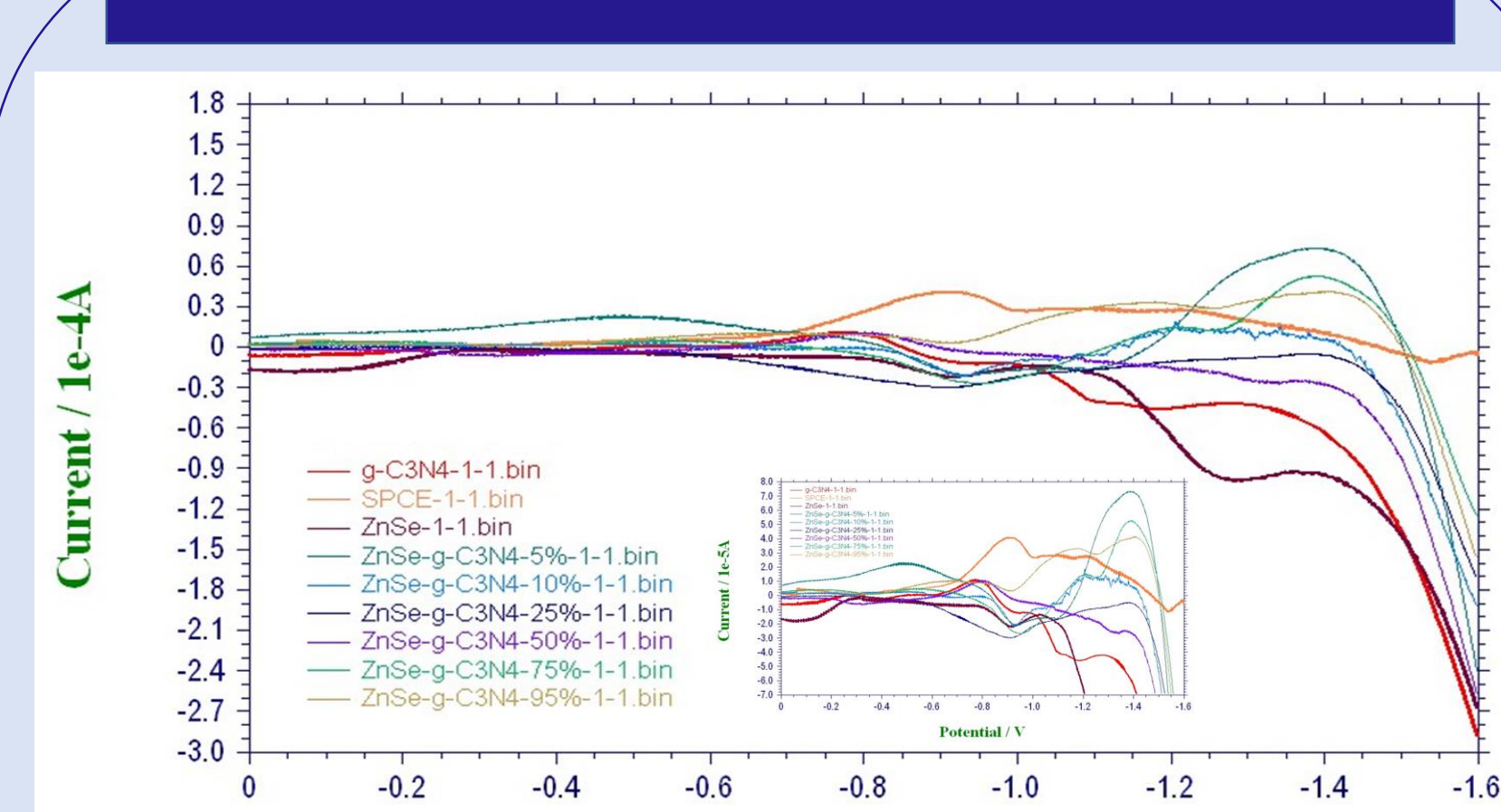


Fig. 14 Cyclic voltammetry of Na₂CO₃ reduction using bare SPE and SPE coated with ZnSe, g-C₃N₄, and ZnSe/g-C₃N₄.

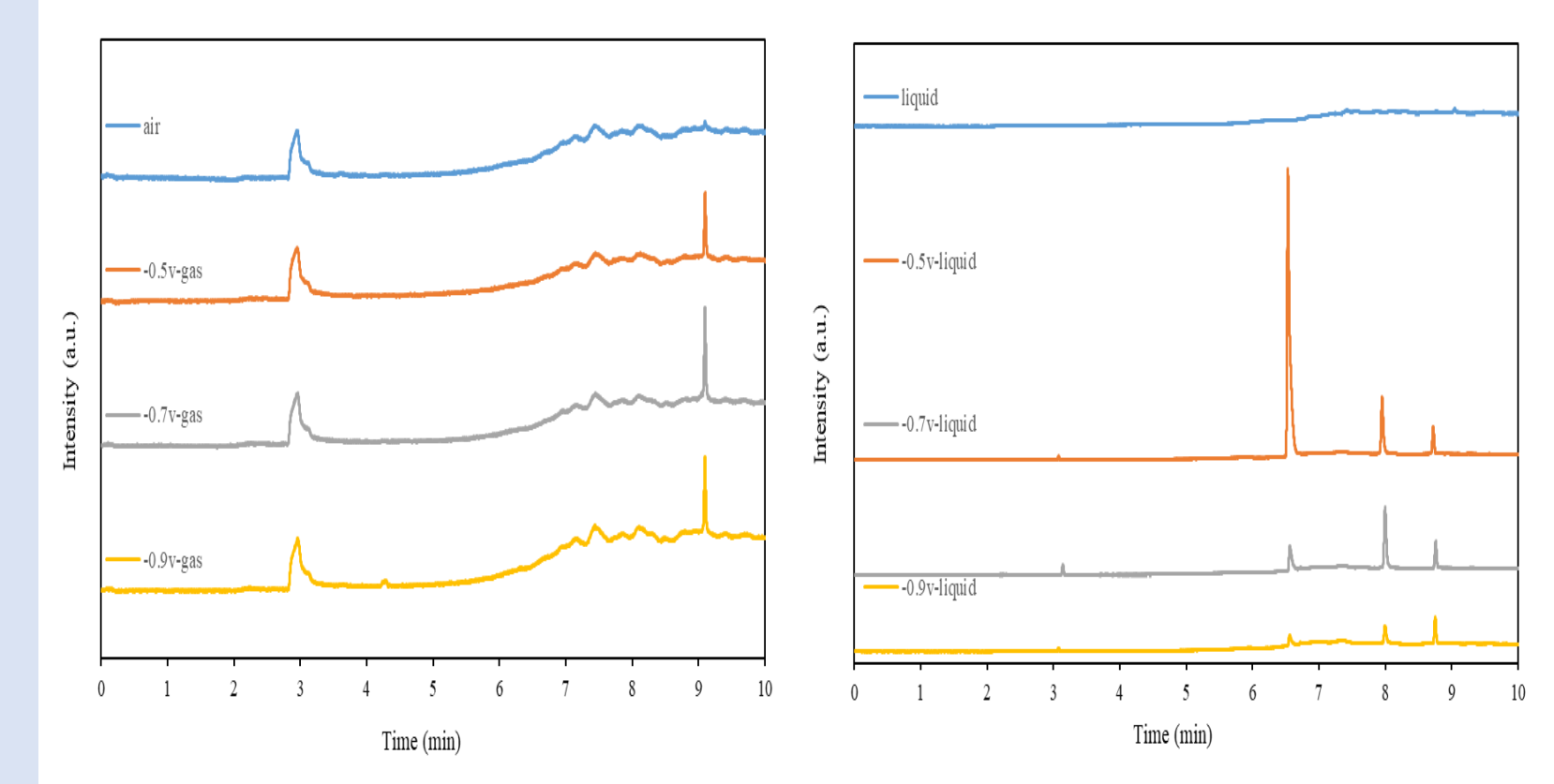


Fig. 15 GC/FID chromatograms of headspace gas and electrolyte solutions obtained during electrocatalytic ZnSe/g-C₃N₄-5wt% reduction of CO₂ using different potentials -0.5V, -0.7V and -0.9V.

EPR

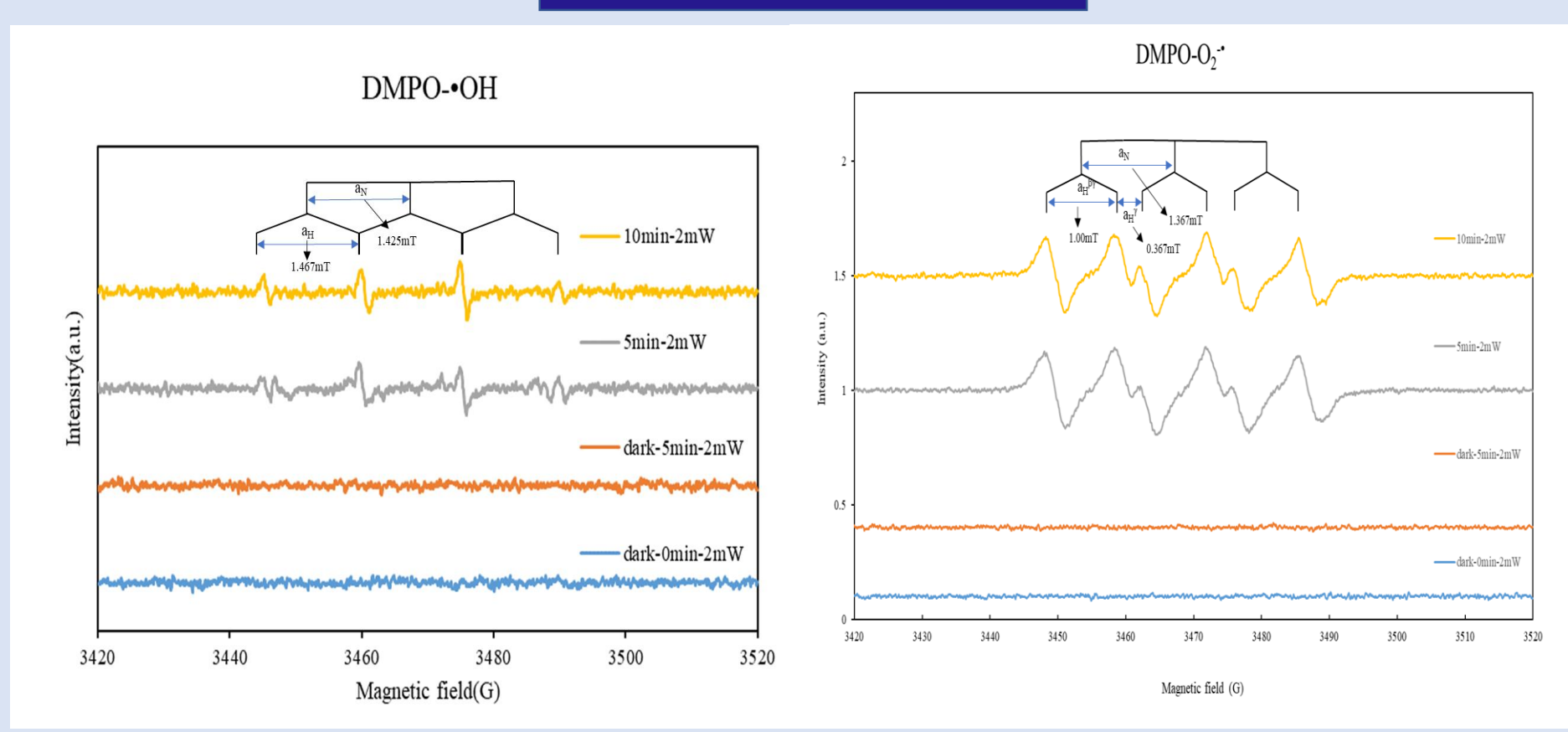


Fig. 11 EPR pattern of ZnSe/g-C₃N₄-5wt%.

Photoreduction of CO₂

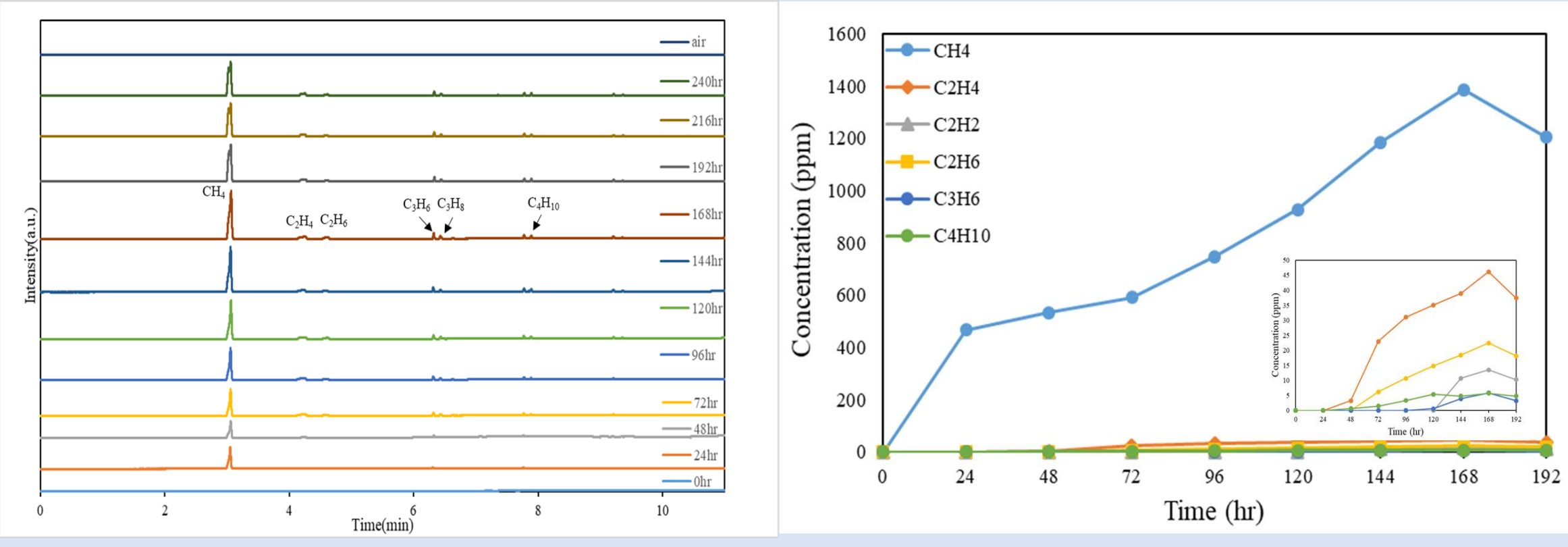


Fig. 12 Photocatalytic reduction of CO₂ as a function of irradiation time over ZnSe/ g-C₃N₄-5wt% .

Mechanism

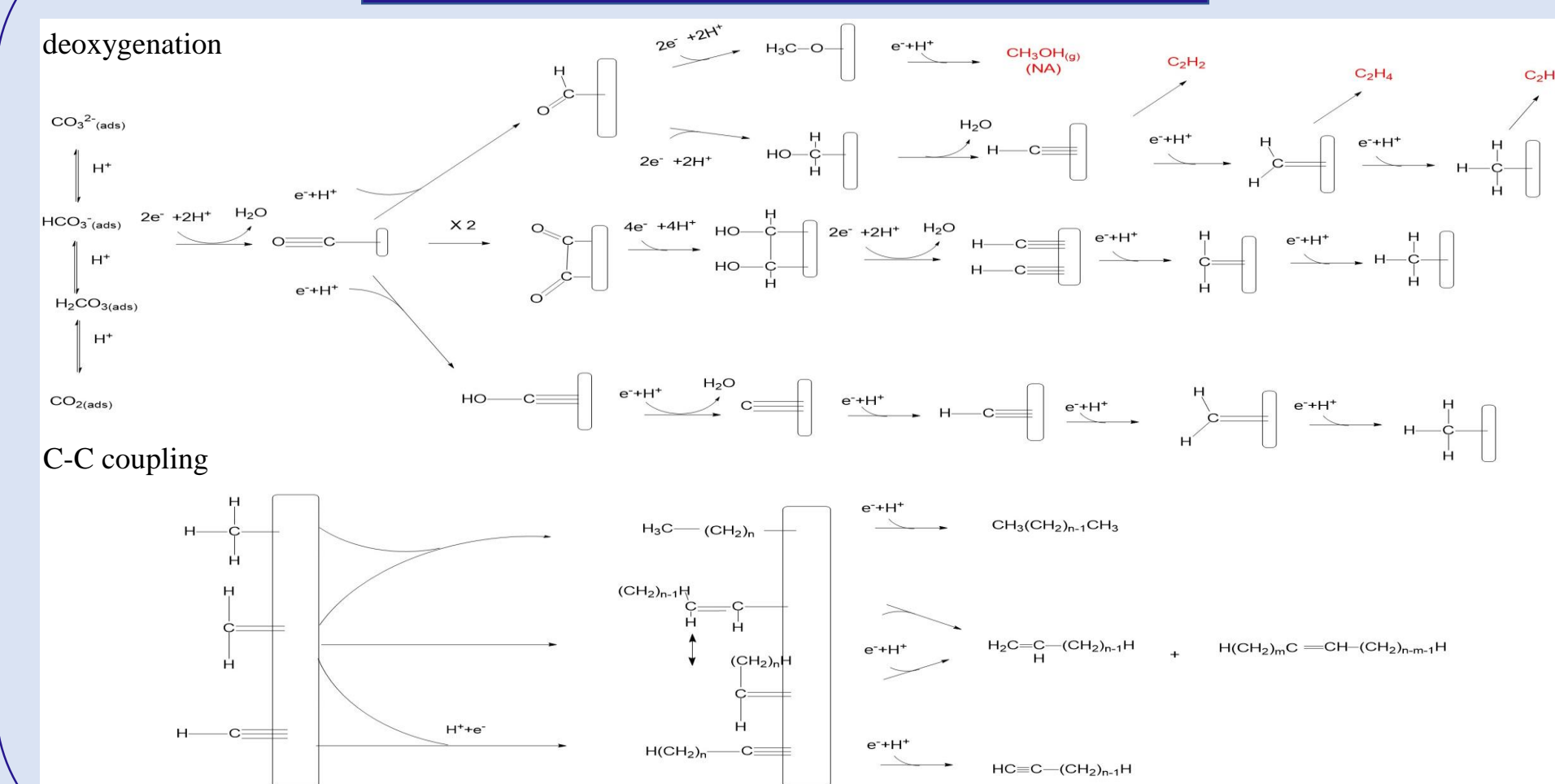


Fig. 13 The pathways for photocatalytic CO₂ reduction.

Summary

The utilization of ZnSe , ZnSe/g-C₃N₄-5wt% for CO₂ reduction and photocatalytic degradation of organic pollutants such as crystal violet (CV) showed remarkable effects, indicating their broad potential in reducing environmental pollution.

Using ZnSe/g-C₃N₄-5wt%, it can be seen that the products that can be obtained under constant potential reduction of CO₂ is acetone.